



## OPEN ACCESS

## EDITED BY

Ryan J. Mailloux,  
McGill University, Canada

## REVIEWED BY

Estela Bevilacqua,  
University of São Paulo, Brazil  
Sumedha Bagga,  
Boston University, United States

## \*CORRESPONDENCE

Sarah A. Wernimont,  
✉ swernimo@umn.edu

RECEIVED 15 February 2023

ACCEPTED 05 May 2023

PUBLISHED 12 May 2023

## CITATION

Nashif SK, Mahr RM, Jena S, Jo S,  
Nelson AB, Sadowski D, Crawford PA,  
Puchalska P, Alejandro EU, Gearhart MD  
and Wernimont SA (2023), Metformin  
impairs trophoblast metabolism and  
differentiation in a dose-  
dependent manner.  
*Front. Cell Dev. Biol.* 11:1167097.  
doi: 10.3389/fcell.2023.1167097

## COPYRIGHT

© 2023 Nashif, Mahr, Jena, Jo, Nelson,  
Sadowski, Crawford, Puchalska,  
Alejandro, Gearhart and Wernimont. This  
is an open-access article distributed  
under the terms of the [Creative  
Commons Attribution License \(CC BY\)](#).  
The use, distribution or reproduction in  
other forums is permitted, provided the  
original author(s) and the copyright  
owner(s) are credited and that the original  
publication in this journal is cited, in  
accordance with accepted academic  
practice. No use, distribution or  
reproduction is permitted which does not  
comply with these terms.

# Metformin impairs trophoblast metabolism and differentiation in a dose-dependent manner

Sereen K. Nashif<sup>1</sup>, Renee M. Mahr<sup>1</sup>, Snehalata Jena<sup>1</sup>, Seokwon Jo<sup>2</sup>,  
Alisa B. Nelson<sup>3</sup>, Danielle Sadowski<sup>1</sup>, Peter A. Crawford<sup>3,4</sup>,  
Patrycja Puchalska<sup>3</sup>, Emilyn U. Alejandro<sup>2</sup>, Micah D. Gearhart<sup>1</sup> and  
Sarah A. Wernimont<sup>1,3\*</sup>

<sup>1</sup>Department of Obstetrics, Gynecology and Women's Health, University of Minnesota, Minneapolis, MN, United States, <sup>2</sup>Department of Integrative Biology and Physiology, University of Minnesota Medical School, Minneapolis, MN, United States, <sup>3</sup>Division of Molecular Medicine, Department of Medicine, University of Minnesota, Minneapolis, MN, United States, <sup>4</sup>Department of Biochemistry, Molecular Biology and Biophysics, University of Minnesota, Minneapolis, MN, United States

Metformin is a widely prescribed medication whose mechanism of action is not completely defined and whose role in gestational diabetes management remains controversial. In addition to increasing the risk of fetal growth abnormalities and preeclampsia, gestational diabetes is associated with abnormalities in placental development including impairments in trophoblast differentiation. Given that metformin impacts cellular differentiation events in other systems, we assessed metformin's impact on trophoblast metabolism and differentiation. Using established cell culture models of trophoblast differentiation, oxygen consumption rates and relative metabolite abundance were determined following 200  $\mu$ M (therapeutic range) and 2000  $\mu$ M (supra-therapeutic range) metformin treatment using Seahorse and mass-spectrometry approaches. While no differences in oxygen consumption rates or relative metabolite abundance were detected between vehicle and 200  $\mu$ M metformin-treated cells, 2000  $\mu$ M metformin impaired oxidative metabolism and increased the abundance of lactate and TCA cycle intermediates,  $\alpha$ -ketoglutarate, succinate, and malate. Examining differentiation, treatment with 2000  $\mu$ M, but not 200  $\mu$ M metformin, impaired HCG production and expression of multiple trophoblast differentiation markers. Overall, this work suggests that supra-therapeutic concentrations of metformin impair trophoblast metabolism and differentiation whereas metformin concentrations in the therapeutic range do not strongly impact these processes.

## KEYWORDS

metformin, metabolism, trophoblast stem cell, BeWo, cytotrophoblast, syncytiotrophoblast, differentiation, mitochondria

## Introduction

Metformin (1,1-dimethylbiguanide) is a first-line treatment for patients with type 2 diabetes given its ability to improve glucose levels, support weight loss, and reduce cardiovascular morbidity (Maruthur et al., 2016). Until recently, metformin was also considered a first-line medication for gestational diabetes mellitus (GDM), improving glucose levels, maternal weight gain, and preeclampsia (Liang et al., 2017; ACOG Practice Bulletin No, 2018; D'Ambrosio et al., 2019; ElSayed et al., 2023). However, metformin is no longer considered a first-line medication for GDM since long-term

follow-up has demonstrated increased weight, body mass index, and adiposity at mid-childhood following *in utero* metformin exposure (Tarry-Adkins et al., 2019). Despite these concerns, there continues to be interest in the use of metformin in pregnancy for potential preeclampsia prevention, reduced maternal weight gain in obese pregnancies, and lower miscarriage rate among pregnancies complicated by polycystic ovarian syndrome (Syngelaki et al., 2016; Løvvik et al., 2019; Adams et al., 2022). However, the mechanisms underlying these potential beneficial outcomes remain unknown.

During pregnancy, the placenta grows to support the health of the developing fetus (Turco and Moffett, 2019). A key cell facilitating nutrient transport to the developing fetus is the syncytiotrophoblast, a unique multi-nucleated cell that supports nutrient transport and gas exchange between maternal and fetal circulation. During the course of pregnancy, cytotrophoblasts divide and fuse to support the development and health of the syncytiotrophoblast (Costa, 2016; Renaud and Jeyarajah, 2022). Trophoblast differentiation is critical for placental development and fetal health. Delayed villous maturation, the most common histopathologic finding in GDM, is associated with poor birth outcomes (Higgins et al., 2011; Treacy et al., 2013; Huynh et al., 2015; Khong et al., 2016; Jaiman et al., 2020). A key finding in delayed villous maturation is an increase in the ratio of cytotrophoblasts to syncytiotrophoblasts, suggestive of potential defects in trophoblast differentiation (Khong et al., 2016). In one limited study, metformin treatment was found to normalize placental histology in pregnancies complicated by GDM (Arshad et al., 2016). However, it is unclear if this is due to improved blood glucose levels or the direct impact of metformin on placental development.

Despite its wide clinical use, metformin's mechanisms of action are not fully understood, and metformin may have unique impacts within distinct tissues (Rena et al., 2017; Aye et al., 2022). Metformin inhibits complex I of the electron transport chain in a dose-dependent manner leading to changes in nucleotide energy charges: this decrease in ATP to ADP and ATP to AMP ratios leads to the activation of AMPK (LaMoia and Shulman, 2021). However, AMPK-independent mechanisms are also postulated to contribute to improved glycemic profiles (Rena et al., 2017). Impacts of metformin on complex I are demonstrated with supra-therapeutic concentrations, in the 1–5 mM range (LaMoia and Shulman, 2021). In contrast, following oral administration, metformin tissue levels are estimated to achieve levels of 50–100  $\mu\text{M}$  (LaMoia and Shulman, 2021). Recent work suggests that maternal and placental metformin concentrations from GDM patients at the time of delivery may be even lower (Tarry-Adkins et al., 2022a). While the timing of metformin administration relative to blood collection is not clear in this study, maternal serum levels are reported in the 0–5  $\mu\text{M}$  range and are linearly correlated to placental metformin levels. This is significantly lower than the 1–5 mM range thought to directly inhibit complex I, suggesting other mechanisms may underlie metformin's impact in pregnancy (Aye et al., 2022).

Mitochondria regulate cellular differentiation in multiple systems, and metformin has been found to promote differentiation in some systems and inhibit it in others (Folmes and Terzic, 2016; Lisowski et al., 2018; Jiang and Liu, 2020; Chakrabarty and Chandel, 2021). Specifically, metformin promotes myogenic, neuronal, and osteogenic differentiation

through impacts on AMPK (Wang et al., 2012; Dadwal et al., 2015; Senesi et al., 2016). Conversely, metformin inhibits differentiation of cancer stem cells in gastric cancer, osteosarcoma, and breast cancers (Cheung et al., 2019; Tan et al., 2019; Zhao et al., 2019). The impact of metformin on trophoblast differentiation has not been reported.

Given the ongoing interest in metformin for the clinical management of obstetric complications and its known impact on cellular differentiation in other systems, we hypothesized that metformin regulates trophoblast differentiation and cellular metabolism. In this work, we employ cell culture models to test the impact of metformin at therapeutic and supra-therapeutic concentrations on trophoblast metabolism and differentiation. While supra-therapeutic doses of metformin impair cellular metabolism and trophoblast differentiation, no significant impact was seen at therapeutic concentrations.

## Materials and methods

**Ethics:** This study does not meet criteria for human subjects research, confirmed by the University of Minnesota Institutional Review Board (HRD # STUDY00014203).

## Cell culture and reagents

BeWo cells were purchased from ATCC and maintained in culture with equal parts F12K (ATCC) (supplemented with 10% Fetal Bovine Serum (R&D Systems), Penicillin-Streptomycin (Gibco)) and DMEM Complete (4.5 g/L glucose, Gibco) (supplemented with Glutamine (Gibco), Sodium Pyruvate (Gibco), 10% Fetal Bovine Serum (Gibco), and Penicillin-Streptomycin (Gibco)). To induce syncytialization, BeWo cells were cultured on tissue-culture treated plates for 24 h. Forskolin (Millipore Sigma) (40  $\mu\text{M}$ ) was added for 48 h with DMSO (0.4%) (Sigma-Aldrich) as the vehicle control. Metformin (Cayman) at concentrations of 200  $\mu\text{M}$  or 2000  $\mu\text{M}$  was added for 72 h. PBS (Gibco) was used as a vehicle control for metformin. Media and treatments were replaced every 24 h during syncytialization.

Trophoblast Stem Cells (TSC) (CT29, Acquired from RIKEN Cell Bank) were maintained in a self-renewing state on iMatrix511 (Amsbio) coated plates in TS Complete media. TS Complete media is comprised of DMEM/F12 media (Gibco) containing 100  $\mu\text{g}/\text{mL}$  primocin, 0.15% BSA, 1% ITS-X, 1% Knockout Serum Replacement and 0.2 mM ascorbic acid and supplemented with 2.5  $\mu\text{M}$  Y27632, 25 ng/mL EGF, 0.8 mM Valproic Acid, 5  $\mu\text{M}$  A83-01, and 2  $\mu\text{M}$  CHIR99021 (Okoe et al., 2018). Cells were cultured at 37°C, 5% CO<sub>2</sub>. On day 0, cells were plated on a 6-well plate coated with iMatrix511 in TS Complete media and metformin (Cayman) at concentrations of 200  $\mu\text{M}$  or 2000  $\mu\text{M}$ . PBS (Gibco) was used as a vehicle control. On day 1, to induce syncytialization, TS Complete media was replaced with ST Differentiation media containing DMEM/F12 with 100  $\mu\text{g}/\text{mL}$  Primocin, 0.1% BSA, 1% ITS-X, 2.5  $\mu\text{M}$  Y27632, 4% KSR, and 2  $\mu\text{M}$  forskolin. Metformin at the respective concentrations was also added during the media change. Self-renewing cells were maintained in TS Complete media with metformin or PBS. On day 4 after plating, RNA was isolated for qPCR.

## Protein expression

Cells were washed with ice-cold PBS and lysed with RIPA Buffer (Sigma) supplemented with Protease Inhibitors (Thermo Fisher Scientific), phosphatase inhibitor cocktail (Pierce), and 1 mM DTT (Sigma) in a 6-well plate. Lysate was then centrifuged for 10 min at 4°C at 21,000Xg. Pierce Bicinchoninic Acid Protein Assay Kit (Thermo Scientific) was used to determine protein concentration. 30 µg of protein per well was used to detect protein expression levels. Lysates were run on 4%–12% Bis-Tris gel (Invitrogen), transferred to PVDF, and blocked with 5% milk (Research Products International). Blots were stained overnight at 4°C with total AMPK (Cell Signaling Technology) and pAMPK Thr 172 (Cell Signaling Technology) antibodies in 2% bovine serum albumin (Gemini Bio). Blots were washed with Tris-Buffered Saline and stained with peroxidase-conjugated secondary antibodies (Jackson ImmunoResearch). Blots were developed using SuperSignal West Pico PLUS Chemiluminescent Substrate (Thermo). Total protein loading was assessed by BlotFastStain (G-Biosciences). Blots were imaged using the Bio-Rad ChemiDoc MP imaging system and band density was quantified using ImageJ.

## Seahorse assay

30,000 BeWo cells were plated into wells of Cell-Tak-coated XFe96 plates containing 100 µL/well of equal parts F12K (ATCC) and DMEM (Gibco). Cells were plated in the presence of PBS, 200 µM metformin, or 2000 µM metformin, and treated with DMSO or 40 µM forskolin 24 h after plating. 72 h after plating, A Seahorse XF cell Mito stress test was performed to measure ECAR and OCR using the Seahorse Extracellular Flux (XFe96) Analyzer (Seahorse Bioscience Inc. North Billerica, MA). On the day of the assay, the media was switched to 180 µL of Seahorse XF assay media (DMEM) freshly supplemented with 16 mM glucose, 10 mM sodium pyruvate, and 2 mM glutamine (Agilent, Santa Clara, CA). The plate was incubated in a 37°C non-CO<sub>2</sub> incubator for 1 h prior to measurement. The plate was then transferred to the Seahorse XFe96 Analyzer (Seahorse Bioscience Inc. North Billerica, MA) for analysis. Once in the instrument, cells underwent measurement of basal oxygen consumption and extracellular acidification, followed by successive treatments with oligomycin A (2 µM), FCCP (carbonyl cyanide-*p*-trifluoromethoxyphenylhydrazone) (1 µM), and rotenone and antimycin A (0.5 µM). OCR and ECAR measurements were normalized per well to DNA, measured using the Quant-iT PicoGreen dsDNA Assay kit. For analysis, post-rotenone/antimycin A OCR readings were subtracted from the rest of OCR values to set baseline mitochondrial respiration. Key bioenergetic parameters (basal respiration, ATP-linked respiration, maximal respiration, spare capacity, and proton leak) from the Mito stress test were calculated according to the manufacturer's protocol (Figure 2B).

## Metabolomics

250,000 BeWo cells were plated on 6-well plates, treated with vehicle or metformin, and 24 h after plating, treated with DMSO or 40 µM forskolin as above. A mirror plate was made to facilitate the normalization of metabolite abundance to total protein. 72 h after plating, samples were collected by washing twice with ice-cold PBS, once in ice-cold water, and

snap-freezing in liquid nitrogen prior to transferring cells in methanol to a fresh tube. The solvent was evaporated and samples were stored at –80°C until ready for metabolite extraction and analysis.

## Relative abundance of glycolytic and TCA cycle intermediates

To determine the relative abundance of selected TCA cycle and glycolytic metabolites, metabolites were extracted as previously described (Ivanisevic et al., 2013; Puchalska et al., 2018; Puchalska et al., 2019), with modifications. Briefly, 1,000 µL of 2:2:1 Acetonitrile (AcN):Water (H<sub>2</sub>O):MeOH (v:v:v) was added to each sample, which underwent three rounds of vortexing, sonication, and snap freezing in liquid nitrogen. The samples were incubated at –20°C for 1–4 h, spun to remove proteins, transferred to fresh tubes, evaporated, and reconstituted in 40 µL of 1:1 AcN:H<sub>2</sub>O. All analyses were performed on a Thermo Vanquish liquid chromatograph with Thermo Q-Exactive Plus mass spectrometer equipped with a heated ESI (HESI) source.

Samples were analyzed using negative mode on an Atlantis Premier BEH Z-HILIC Column (2.1 mm × 100 mm, 1.7 µm). Separation was completed using gradients of Mobile phase A (15 mM ammonium bicarbonate in water, pH 9.0) and Mobile Phase B (15 mM ammonium bicarbonate pH, 9.0 with 90% AcN). Binary gradients included 10% Mobile Phase A for 5 min, 35% Mobile Phase A for 2 min, and 10% Mobile Phase A for 3 min. Separations were performed at a flow rate of 0.5–1 mL/min and column temperature at 30°C with an injection volume of 2 µL. The mass spectrometer was operated in negative mode using full scan (FS) mode (*m/z* 68–1,020) with optimized HESI source conditions: auxiliary gas 10, sweep gas 1, sheath gas flow at 30 (arbitrary unit), spray voltage –4 kV, capillary temperature 350°C, S-lens RF 50, and auxiliary gas temperature 350°C. The automatic gain control (AGC) target was set at 3e6 ions with a resolution of 70,000.

Xcalibur's QuanBrowser from Thermo was used for peak identification and integration. Metabolite profiling data was analyzed using verified peaks and retention times. Metabolite peak identity was confirmed based on retention time, *m/z*, and compared to authentic standards as described previously (Puchalska et al., 2018; Puchalska et al., 2019). The integrated signal for each metabolite was normalized to total protein determined using Bicinchoninic Acid Assay (BCA) on mirror plates for each condition.

## HCG production

After treatment, media was collected and samples were tested for alpha-HCG using ELISA assay (DRG International). DMSO-treated samples were diluted (1:2) with PBS and Forskolin-treated samples were diluted (1:100). HCG expression was detected using the Gen5 program via the Synergy HTX Multimode Reader (BioTek).

## Analysis of mRNA expression

Cells were washed with ice-cold PBS. Total RNA was extracted from cells using the Quick RNA Mini-Prep Extraction Kit (Zymo

TABLE 1 Key Resources

Reagent or Resource	Source	Identifier
<b>Cell Lines</b>		
BeWo Cell Line	ATCC	CCL-98
Trophoblast Stem Cells	Riken BRC	RCB4937:CT-29
<b>Antibodies</b>		
pAMPK	Cell Signaling Technologies	#2531S
AMPK	Cell Signaling Technologies	#2532S
HRP conjugated Anti-Rabbit antibody	Jackson ImmunoResearch	111-035-003
HRP conjugated Anti-Mouse antibody	Jackson ImmunoResearch	115-035-003
Mouse eCadherin	BD Transduction	610181
Monoclonal HCG	Abcam	ab238319
Alexa Fluor 488	Abcam	ab150117
Alexa Fluor 647	Abcam	ab150083
<b>Chemicals</b>		
DMEM High Glucose	Gibco	11965118
F12K	ATCC	30-2004
Fetal Bovine Serum	Atlanta Biologicals	S11150
Penicillin-Streptomycin	Gibco	15140-122
Sodium Pyruvate	Gibco	11360-070
DMSO	Sigma	D2650
Forskolin	Sigma	F-6886
PBS	Gibco	14190
Metformin	Cayman	13118
Paraformaldehyde	Thermo Scientific	043368-9M
TritonX	Fisher Bioreagents	BP151
Goat Serum	R&D Systems	S13150
Mounting Media with NucBlue	Invitrogen	P36981
Poly-L-Lysine	Sigma	P4707
RIPA Buffer	Sigma	R0278
Protease Inhibitor Cocktail	Sigma	P8340
HCG ELISA Kit	DRG International	EIA-1469R
Quick-RNA MiniPrep Kit	Zymo Research	R1055
Supermix for RT-qPCR	Bio-Rad	1708841
Sybr Green Supermix	Bio-Rad	1725274
<b>Oligonucleotides</b>		
Hs-CGA-Forward	IDT	TGTGCAGGATTGCCAGAAT
Hs-CGA-Reverse	IDT	TGGACCTTAGTGGAGTGGGA
Hs-CGB2-Forward	IDT	GGGACATGGGCATCCAAGG
Hs-CGB2-Reverse	IDT	GCACGCGGGTCATGGT

(Continued on following page)

TABLE 1 (Continued) Key Resources

Reagent or Resource	Source	Identifier
Hs-HSD11B2-Forward	IDT	TGACCAAACCAGGAGACATTA
Hs-HSD11B2-Reverse	IDT	CGCATCAGCAACTACTTCATTG
Hs-ERVW-1-Forward	IDT	CCATGCCGCTGTATGACCAG
Hs-ERVW-1-Reverse	IDT	GGGTTCCTTAGAAAGACTCCT
Hs-ERVFRD-1-Forward	IDT	CGGATACCTTCCCTAGTGCCAT
Hs-ERVFRD-1-Reverse	IDT	ACAGCTTCACTTGGGTGTGA
Hs-TEAD4-Forward	IDT	CAGTATGAGAGCCCCGAGAA
Hs-TEAD4-Reverse	IDT	TGCTTGAGCTTGTGGATGAA
Hs-OVOL1-Forward	IDT	CCGTGCGTCTCCACGTGCAA
Hs-OVOL1-Reverse	IDT	GGCTGTGGTGGGCAGAAGCC
Hs-Cyclophilin-Forward	IDT	GGAGATGGCACAGGAGGAAA
Hs-Cyclophilin-Reverse	IDT	GCCCGTAGTGCTTCAGTTT
Hs-SLC38A1-Forward	IDT	CATCGCCTTTTGCCACCTTT
Hs_SLC38A1-Reverse	IDT	GGAAGCTTGACACCCCTGTT
Hs-SLC38A2-Forward	IDT	AGCTGCTCTGAAAAGCCAT
Hs-SLC38A2-Reverse	IDT	GCCCACAATGCGATTGCTC
Hs-SLC7A5-Forward	IDT	GCTCATCATCCGGCCTTCA
Hs-SLC7A5-Reverse	IDT	GAGCAGCAGCACGCAG
Hs-SLC7A8-Forward	IDT	CCAGGCACCGAAACAACACC
Hs-SLC7A8-Reverse	IDT	GAGCCGATGATGTTCCCTACGAT
Hs-SLC27A6-Forward	IDT	CTAGTGGTGGGCGCAGATT
Hs-SLC27A6-Reverse	IDT	GCTCATCAGGTGAGGTGCTC

Research). Equal amounts of RNA were used to synthesize cDNA (BioRad). For quantitative real-time PCR, reactions were carried out using SsoAdvanced Universal SYBR Green Supermix (BioRad) on a CFX384 Real-Time System (Bio-Rad). Transcripts were quantified using the  $2^{-\Delta\Delta CT}$  method and normalized to cyclophilin. See Key Resources Table 1 for specific primers.

## Imaging

50,000 BeWo cells were plated on poly-L-lysine pre-treated glass coverslips along with media containing PBS vehicle or 200  $\mu$ M or 2000  $\mu$ M metformin. 24 and 48 h after plating, DMSO or 40  $\mu$ M forskolin was applied. 72 h after plating coverslips were fixed with 4% paraformaldehyde (Fisher Scientific) for 10 min and then permeabilized using 0.1% TritonX for 10 min. After washing, coverslips were blocked for 1 h with 5% goat serum in PBS. Coverslips were stained overnight at 4°C with HCG (Abcam) and eCadherin (BD Biosciences) antibodies. The following day, coverslips were washed three times, then incubated at room temperature with mouse (Jackson ImmunoResearch) and rabbit (Jackson ImmunoResearch) secondary antibodies. Coverslips were again washed and mounted on glass slides using mounting media with Prolong

Glass Antifade Mountant with NucBlue nuclear Stain (Invitrogen). Images were acquired on an Olympus FluoView BX2 Upright Confocal microscope at the University of Minnesota Imaging Core. Fusion index was quantified as the number of nuclei in syncytia divided by the total number of nuclei using Fiji.

## Quantification and statistical analysis

Statistical outliers were excluded following identification by the Grubbs test. ANOVA was used to compare the means of more than two groups. *p* values less than 0.05 were considered statistically significant. Data were analyzed using GraphPad Prism.

## Results

### Metformin treatment increases phospho-AMPK signaling in BeWo cells

The BeWo cell line is an established model system where forskolin, an adenylate cyclase activator upstream of protein

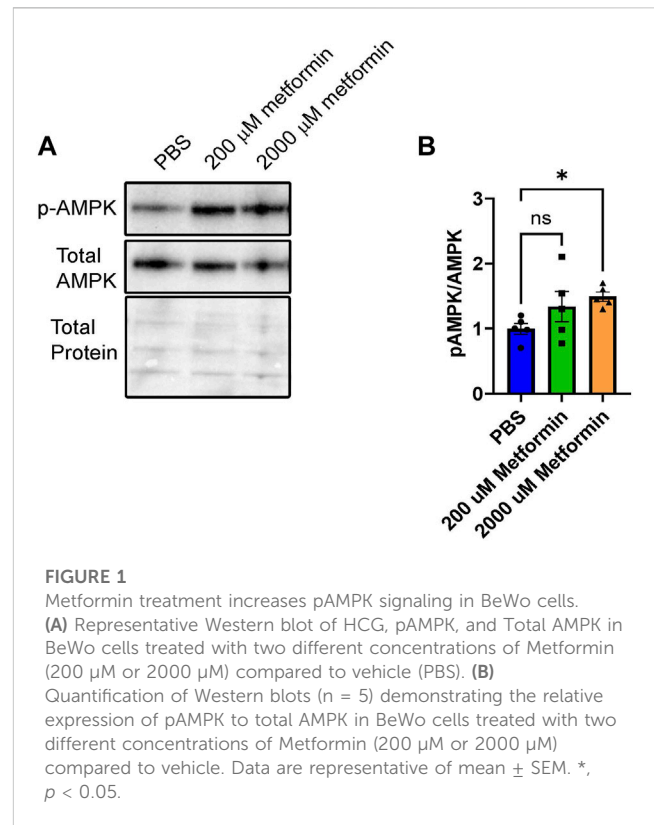
kinase A, induces both biochemical and morphologic syncytialization (Orendi et al., 2011; Rothbauer et al., 2017). These differentiation parameters are detected through the production of human chorionic gonadotrophin (HCG) and coordinated changes in gene transcription along with the fusion of cell membranes resulting in morphologic syncytia (Costa, 2016; Renaud and Jeyarajah, 2022).

Using the BeWo model system, we first validated metformin activity within undifferentiated cells by assessing AMP-activated protein kinase (AMPK) activity. Metformin increases AMPK activity through phosphorylation of Thr172 in the activation loop of the kinase domain (Musi and Goodyear, 2002). Following treatment of BeWo cells with vehicle (PBS), 200  $\mu$ M metformin, or 2000  $\mu$ M metformin for 72 h, phosphorylation of AMP-activated protein kinase (pAMPK at Thr172) relative to total AMPK was detected by Western blotting (Figures 1A, B). Upon treatment with 200  $\mu$ M metformin, a trending but statistically insignificant increase in pAMPK at Thr172 was observed. However, 2000  $\mu$ M metformin, increased pAMPK at Thr172 compared to total AMPK. This overall suggests that metformin enters BeWo cells and increases AMPK activity at the 2000  $\mu$ M concentration.

## Metformin's impact on oxidative and glycolytic metabolism

Prior work demonstrates that cytotrophoblasts and syncytiotrophoblasts differ in their glycolytic and oxidative metabolism (Kolahi et al., 2017; Bucher et al., 2021). Given this, we tested the impact of metformin on undifferentiated and differentiated trophoblast metabolism. BeWo cells were plated in the presence of vehicle (PBS), 200  $\mu$ M or 2000  $\mu$ M metformin. 48 h after inducing differentiation with forskolin, a Seahorse Mitochondrial Stress Assay was performed to measure how metformin impacts the oxygen consumption rate (OCR) following the sequential addition of inhibitors as depicted in Figures 2A, B. Forskolin treatment decreases basal respiration, ATP-linked respiration, maximum respiration, and spare capacity compared to DMSO-treated control cells (Figures 2C–F). However, no differentiation-dependent change in proton leak or non-mitochondrial respiration was detected. Differentiation in the presence of 200  $\mu$ M metformin similarly decreased forskolin-dependent basal respiration, ATP-linked respiration, maximum respiration, and spare capacity with no differences detected between vehicle and 200  $\mu$ M metformin OCR. In contrast, differentiation in the presence of 2000  $\mu$ M metformin profoundly decreased basal, ATP-linked, maximal, and non-mitochondrial respiration compared to vehicle treatment. Overall, this demonstrates that 2000  $\mu$ M metformin, not 200  $\mu$ M metformin, has a broad impact on oxidative metabolism (Figure 2A, C–H).

Extracellular acidification rate (ECAR) serves as a surrogate measure of glycolysis. Given the profound impacts of 2000  $\mu$ M metformin on oxidative metabolism, we determined the impact of metformin on basal ECAR. Forskolin treatment slightly increased basal ECAR rates in PBS and 200  $\mu$ M metformin-treated cells, though no statistically significant differences were detected between groups (Supplemental Figure S1 A, B, D). Following



treatment with 2000  $\mu$ M metformin, ECAR increased significantly in DMSO-treated cells compared to vehicle (Supplemental Figures S1C, D). This is consistent with higher metformin concentrations impairing oxidative phosphorylation and increasing glycolytic rate.

## Metformin's impact on the relative abundance of glycolytic and TCA cycle intermediates

Given the broad differences observed in the OCR with differentiation, we next determined how therapeutic and supra-therapeutic concentrations of metformin impact the relative abundance of cellular metabolites during differentiation. Using a high-resolution liquid chromatography, mass-spectrometry (LC-MS) approach, we determined relative metabolite abundance following treatment of BeWo cells with DMSO or forskolin in the presence of PBS, 200  $\mu$ M or 2000  $\mu$ M metformin. Following differentiation, ATP increased in PBS and 200  $\mu$ M metformin-treated cells (Figure 3A). Surprisingly, 2000  $\mu$ M metformin maintained ATP levels despite the profound impairments found in oxidative phosphorylation (Figure 2), though no differentiation-dependent increase was found. (Figure 3A). This suggests that upon treatment with 2000  $\mu$ M metformin, increased glycolytic activity may preserve overall ATP abundance.

We next examined the impact of metformin on lactate, pyruvate, alanine, and select TCA cycle intermediates (Figures 3B–D). After glucose enters a cell, it undergoes glycolysis resulting in pyruvate which may be metabolized to lactate, alanine, or enter the TCA cycle. Treatment with 2000  $\mu$ M metformin increased lactate and alanine

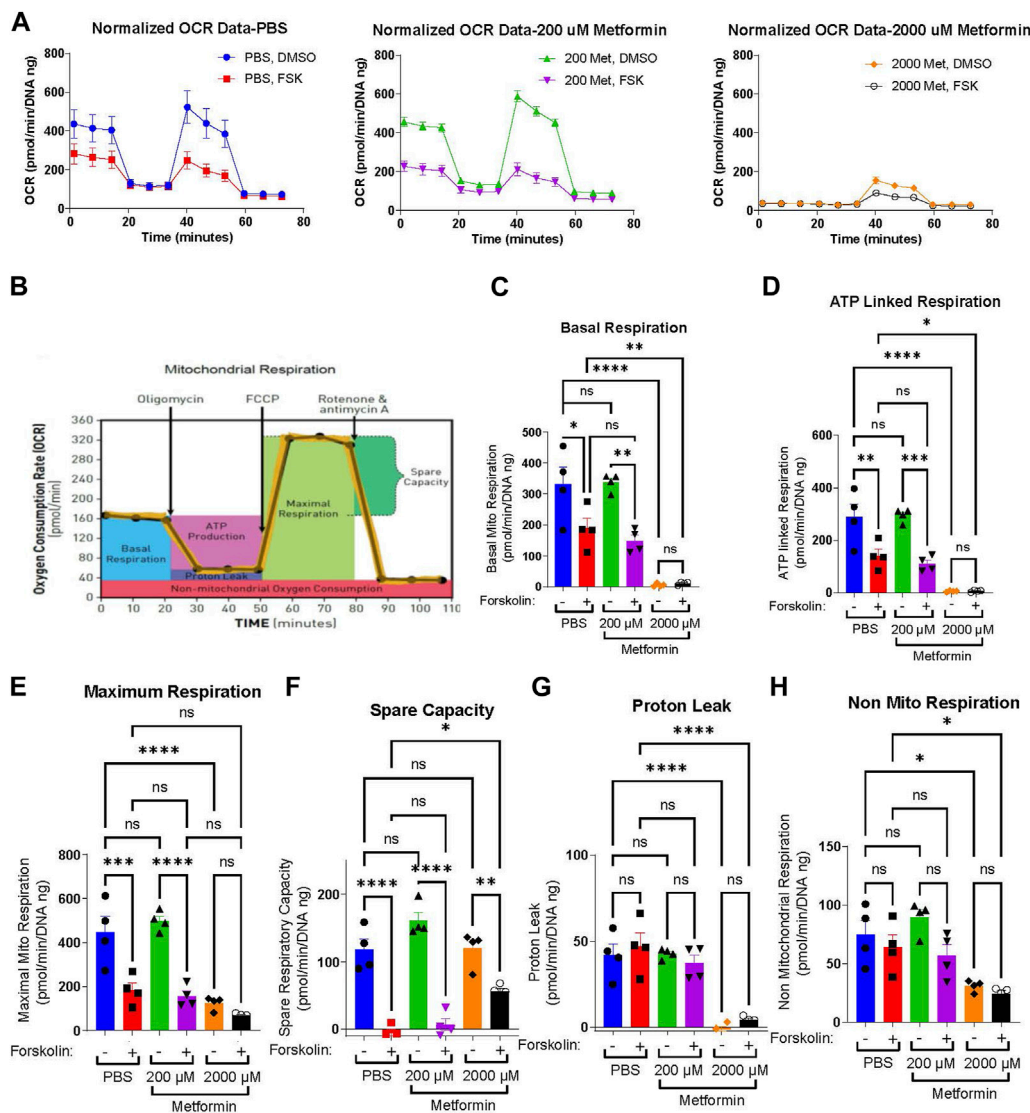


**FIGURE 2**  
 Metformin impairs the oxygen consumption rate at high concentrations (A) Normalized Oxygen Consumption Rate (pmol/min/DNA ng) during mitochondrial flux assay for BeWo cells treated with vehicle, 200 μM metformin, or 2000 μM metformin in the presence of DMSO (0.4%, vehicle) or 40 μM forskolin (FSK) for 48 h. (B) Schematic depicting the impact of sequential inhibitor additions to oxygen consumption rate during Seahorse Mitochondria Stress Test and bio-energetic parameters calculated from the assay. (C–H) Bar graphs representing (C) Basal Mitochondrial Respiration, (D) ATP Linked Respiration, (E) Maximal Respiration, (F) Spare Capacity, (G) Proton Leak and (H) non-mitochondrial respiration (all in (pmol/min/DNA ng)) for vehicle, 200 μM and 2000 μM metformin treated BeWo cells. *n* = 4 biologic replicates. Data are representative of mean ± SEM. \*, *p* < 0.05; \*\*, *p* < 0.01; \*\*\*, *p* < 0.001; and \*\*\*\*, *p* < 0.0001.

abundance compared to PBS and 200 μM metformin treatments (Figure 3C). This is consistent with the observed increase in glycolytic metabolism following 2000 μM metformin treatment.

Differentiation in PBS-treated cells increased citrate, aconitic acid, α-ketoglutarate, and succinate (Figure 3D). This trend persisted in 200 μM treated cells, though a differentiation-dependent increase was only statistically significant for α-ketoglutarate (Figure 3D). In comparison, differentiation following treatment with 2000 μM metformin significantly increased citrate, aconitic acid, α-ketoglutarate, and succinate (Figure 3D). This differentiation-dependent increase in α-ketoglutarate, succinate, and malate with 2000 μM metformin

treatment exceeds that observed following vehicle treatment. This suggests that inhibition of oxidative phosphorylation by supra-therapeutic concentrations of metformin may result in the accumulation of TCA intermediate metabolites due to impairments in oxidative metabolism.

### Impact of metformin on trophoblast differentiation

Mitochondria regulate cellular differentiation events across multiple systems (Folmes and Terzic, 2016; Lisowski et al., 2018;

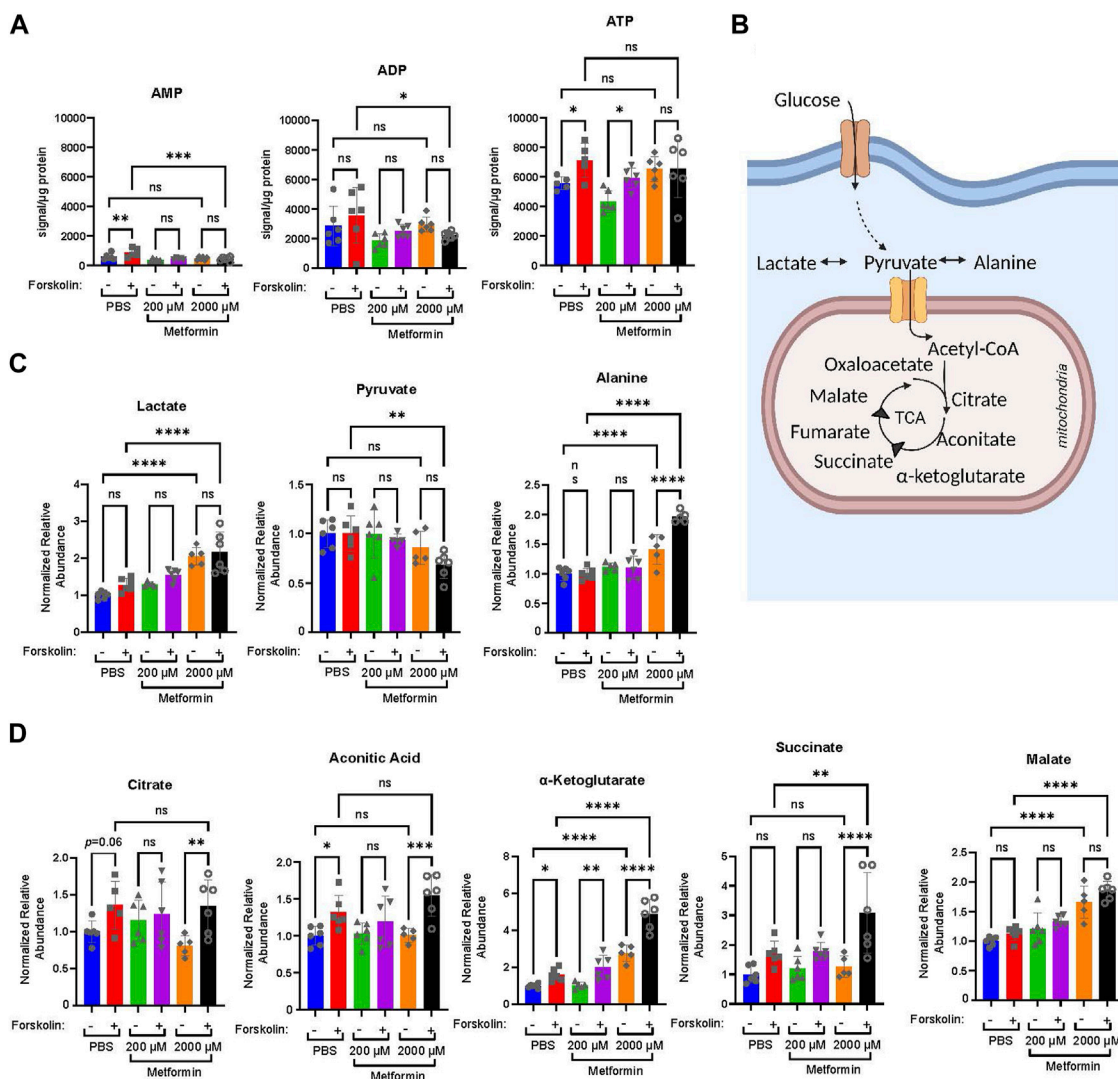


**FIGURE 3**

Metformin impacts the relative abundance of high energy and TCA cycle metabolites. Forty-eight hours following treatment of BeWo cells with DMSO or Forskolin in the presence of vehicle, Metformin 200  $\mu$ M, or Metformin 2000  $\mu$ M, high resolution mass-spectrometry was used to determine the relative abundance of metabolites: **(A)** Normalized abundance of AMP, ADP, and ATP. Data presented are total metabolite signal normalized to  $\mu$ g protein for each condition.  $n = 6$  biologic replicates. **(B)** Schematic demonstrating glucose metabolism to pyruvate, lactate, alanine, and TCA cycle metabolites. **(C)** Normalized relative abundance of lactate, pyruvate, and alanine. Normalized relative abundance is total metabolite signal divided by  $\mu$ g protein for each condition and normalized to DMSO-treated vehicle control.  $n = 6$  biologic replicates. **(D)** Normalized relative abundance of citrate, aconitate,  $\alpha$ -ketoglutarate, succinate, and malate. Data presented are total metabolite signal divided by  $\mu$ g protein for each condition and normalized to DMSO-treated vehicle control. Data are representative of mean  $\pm$  SEM.  $n = 6$  biologic replicates. \*,  $p < 0.05$ ; \*\*,  $p < 0.01$ ; \*\*\*,  $p < 0.001$ ; and \*\*\*\*,  $p < 0.0001$ .

Chakrabarty and Chandel, 2021). To test the impact of metformin on trophoblast differentiation, we plated BeWo cells in the presence of vehicle, 200  $\mu$ M or 2000  $\mu$ M metformin and treated these cells 24 h later with vehicle (DMSO) or forskolin to induce syncytialization. We first assessed the impact of metformin on differentiation by assessing HCG production in media samples. HCG is a peptide hormone made by syncytiotrophoblasts (Fournier et al., 2015). We found significantly lower levels of HCG in media samples obtained from cells treated with 2000  $\mu$ M metformin compared to those in the vehicle control and 200  $\mu$ M metformin groups (Figure 4A), suggestive of differentiation defects with supra-therapeutic metformin treatment.

Trophoblast differentiation requires upregulation of genes necessary to support transcription, synthetic, and fusogenic machinery during trophoblast differentiation (Costa, 2016; Renaud and Jeyarajah, 2022). To test the impact of metformin on this gene reprogramming, we treated BeWo cells with metformin and induced differentiation. In PBS-treated cells, forskolin increased the expression of *CGA* and *CGB2* (involved in HCG production), *HSD11B2* (regulator of glucocorticoid metabolism), *ERVW-1* and *ERVFRD-1* (fusogenic proteins), and *OVOL1* (transcription factor) as expected (Figures 4B–G). Differentiation in the presence of 200  $\mu$ M metformin similarly increased expression of *CGA*, *CGB2*, *HSD11B2*, *ERVFRD-1*, and

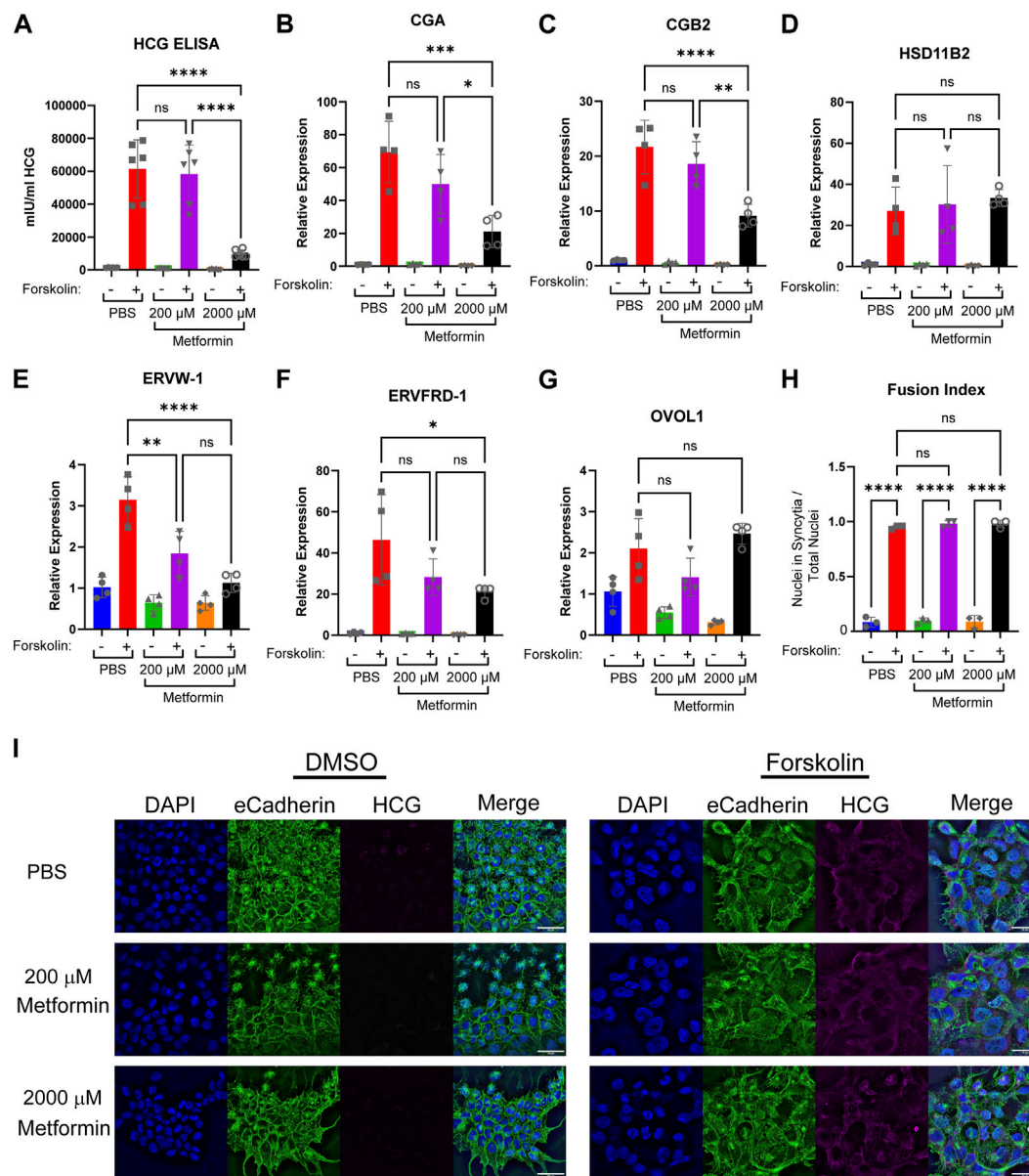
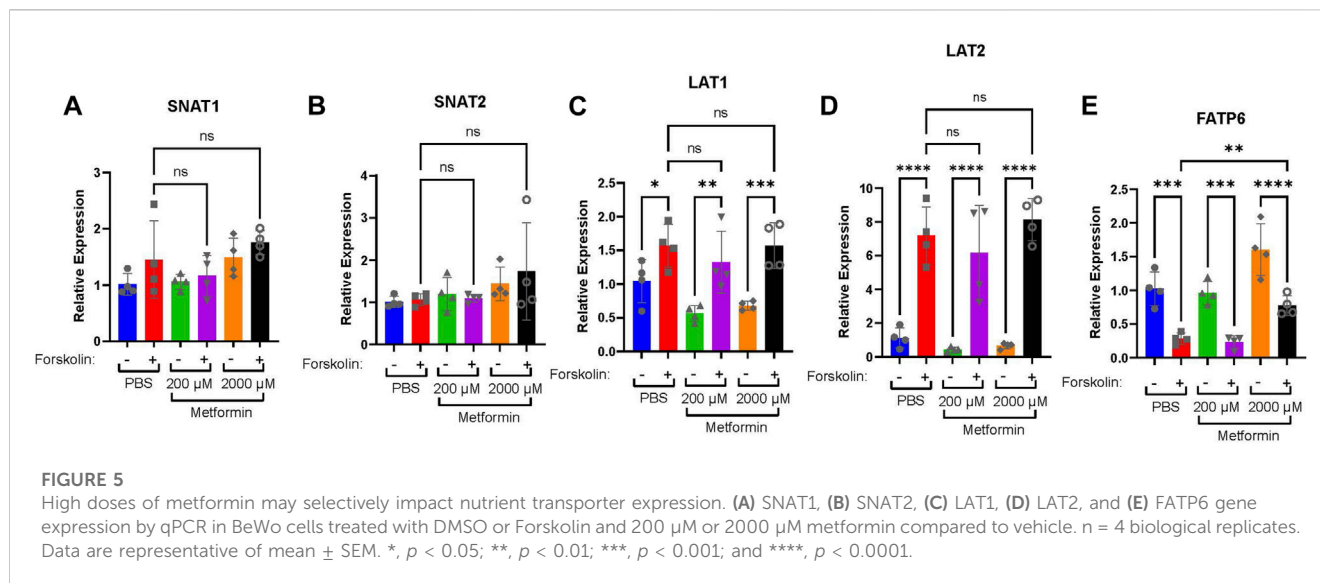


**FIGURE 4** Increasing concentrations of metformin impair biochemical syncytialization. Forty-eight hours following treatment of BeWo cells with DMSO (0.4%) or 40 μM forskolin (FSK) in the presence of vehicle, Metformin 200 μM, or Metformin 2000 μM, we assessed: (A) Production of HCG quantified by ELISA. n = 6 biologic replicates. (B–G) Relative gene expression by qPCR: (B) *CGA*, (C) *CGB2* (D) *HSD11B2* (E) *ERVW-1* (F) *ERVFRD-1* (G) *OVOL1*. n = 4 biological replicates. Data are representative of mean ± SEM. (I) Representative images of nuclear (DAPI, blue), cell membrane (E-cadherin, green), and HCG (magenta) stained BeWo cells treated for 48 h with DMSO or forskolin (FSK) in the presence of vehicle, Metformin 200 μM, or Metformin 2000 μM. Scale bar represents 50 micron. (H) Quantification of fusion index (number of nuclei in syncytia divided by total number of nuclei). n = 6 biologic replicates and 3 fields of view from each replicate. Data are representative of the mean ± SEM. \*, p < 0.05; \*\*, p < 0.01; \*\*\*, p < 0.001; and \*\*\*\*, p < 0.0001.

*OVOL1* (Figure 4C, D, F, G). However, *ERVW-1* expression upon forskolin differentiation was lower (Figure 4E) in the presence of 200 μM of metformin in comparison to PBS. Treatment with 2000 μM metformin impaired forskolin-induced upregulation of *CGA*, *CGB2*, *ERVW-1*, and *ERVFRD-1* in comparison to PBS (Figures 4B, C, E, F). However, no difference in *OVOL1* or *HSD11B2* expression was detected following 2000 μM metformin treatment compared to vehicle (Figures 4D, G). This suggests that 2000 μM metformin may selectively impair transcriptional reprogramming of BeWo cells during differentiation.

To assess morphologic syncytialization, BeWo cells were plated on glass coverslips in the presence of vehicle, 200 or 2000 μM metformin prior to inducing syncytialization. 48 h following differentiation, coverslips were stained with antibodies to HCG, which increases upon differentiation, and E-cadherin, which decreases upon differentiation as membrane fusion occurs (Figure 4I). The degree of fusion was quantified through the fusion index which identifies the number of nuclei found within syncytia divided by the total number of nuclei. We found robust induction of syncytialization upon treatment with forskolin



with >90% of nuclei found in syncytia in control cells. Treatment of BeWo cells with 200 and 2000  $\mu\text{M}$  metformin resulted in similar degrees of syncytialization, with no statistically significant differences noted in the fusion index (Figure 4H). Combined with gene expression data, this suggests that supra-therapeutic metformin treatment may de-couple biochemical and morphologic differentiation, which has been previously described (Cheng, 2004; Orendi et al., 2010; Leduc et al., 2012; Omata et al., 2013).

Given that differentiation regulates the expression of nutrient transporters (Karahoda et al., 2022), we assessed changes in nutrient transporter expression in the presence of metformin. This may reflect a mechanism by which metformin could impact fetal growth. SNAT1 (*SLC38A1*) and SNAT2 (*SLC38A2*) (Figures 5A, B) are involved in the transport of neutral amino acids, and no difference in expression was detected following treatment with 200 or 2000  $\mu\text{M}$  metformin. LAT1 (*SLC7A5*) and LAT2 (*SLC7A8*) (Figure 5 C, D) are involved in the transport of L-amino acids, and following treatment with vehicle, 200 or 2000  $\mu\text{M}$  metformin, a similar forskolin-dependent increase in expression was observed in all investigated groups. Finally, we assessed the expression of FATP6 (*SLC27A6*) (Figure 5E), which is involved in the transport of fatty acids, and observed increased expression following forskolin treatment in cells treated with 2000  $\mu\text{M}$  metformin compared to vehicle control. This suggests that high doses of metformin may selectively impact nutrient transporter expression.

## Impact of metformin on the trophoblast stem cell model of differentiation

While Bewo cells are a widely accepted model of syncytialization, we sought to test the impact of metformin on trophoblast differentiation in another established model system. In the trophoblast stem cell model (Okoe et al., 2018), cytotrophoblasts isolated from first-trimester placenta are maintained in culture in the presence of WNT and EGF activators and TFG-B, histone deacetylase, and ROCK

inhibitors. Syncytialization is induced by removing these WNT, EGF, and HDAC modulators and adding a low dose of forskolin.

In the trophoblast stem cell model, 2000  $\mu\text{M}$  metformin resulted in cell death in both self-renewing (SR) and differentiation (ST) conditions. However, we did not see evidence of cell death at the 200  $\mu\text{M}$  metformin concentration. Comparing the impact of 200  $\mu\text{M}$  metformin to the vehicle, we did not detect any difference in HCG production by ELISA (Figure 6A). No expression differences were observed in *CGA*, *CGB2*, *HSD11B2*, *ERVW-1*, *ERVFRD-1*, or *TEAD4* following treatment with 200  $\mu\text{M}$  metformin compared to vehicle (Figure 6B). This again suggests that therapeutic concentrations of metformin do not dysregulate trophoblast differentiation.

## Discussion

In this work, we evaluated the impact of metformin on trophoblast metabolism and differentiation using established cell culture models of trophoblast differentiation. We found that millimolar doses of metformin inhibited oxidative phosphorylation, resulting in increased glycolysis, lactate, and TCA metabolites. Similar metabolic changes did not occur with 200  $\mu\text{M}$  metformin treatment, consistent with prior reports that therapeutic concentrations of metformin may not function through impairment of Complex I activity. While treatment with 2000  $\mu\text{M}$  of metformin impaired gene expression and HCG production following differentiation, 200  $\mu\text{M}$  of metformin did not result in similar impairments (See Model in Supplemental Figure S2). This overall suggests that therapeutic concentrations of metformin do not impair trophoblast differentiation.

One surprising observation is that supra-physiologic metformin impairs HCG production and broadly impacts the expression of multiple genes involved in trophoblast differentiation: however, we do not detect differences in morphologic syncytialization. Prior studies have identified distinct regulators of biochemical and morphologic syncytialization, including transcription factors and differential activators of protein kinase A, protein kinase C, and mitogen-activated protein kinases (MAPK) pathways (Cheng, 2004;

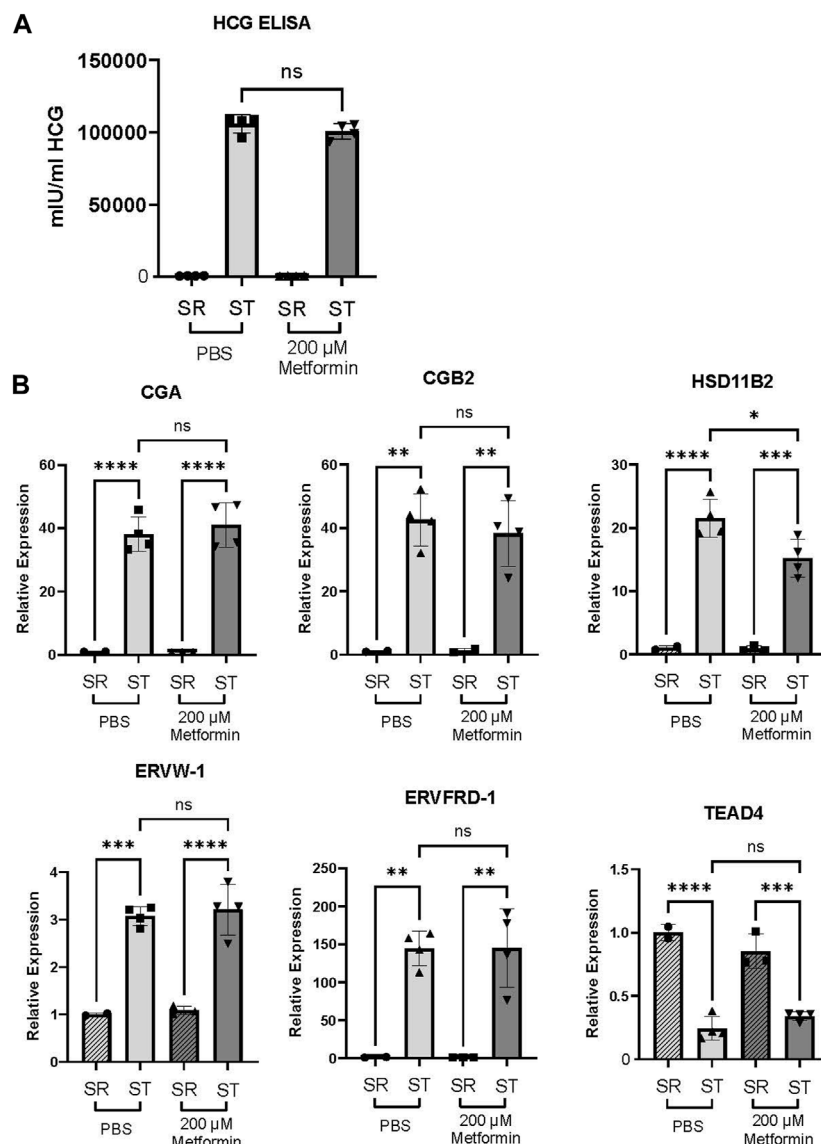


FIGURE 6

Metformin does not impair trophoblast stem cell differentiation. (A) Production of HCG quantified by ELISA in self-renewing (SR) cells or syncytiotrophoblast (ST) Trophoblast stem cells treated with vehicle (PBS) or 200  $\mu$ M metformin.  $n = 6$  biologic replicates. (B) CGA, CGB, HSD11B2, ERVW, ERVFRD, and TEAD4 gene expression by qPCR in SR or ST Trophoblast stem cells.  $n = 4$  biological replicates. Data are representative of mean  $\pm$  SEM. \*,  $p < 0.05$ ; \*\*,  $p < 0.01$ ; \*\*\*,  $p < 0.001$ ; \*\*\*\*,  $p < 0.0001$ .

Orendi et al., 2010; Leduc et al., 2012; Omata et al., 2013). We speculate that supra-physiologic concentrations of metformin may impact the expression or activation of specific transcription factors or signaling pathways that distinctly regulate biochemical and morphologic differentiation. Future work will be directed toward delineating this distinction.

Despite its widespread clinical use, metformin's mechanism of action is not completely defined (LaMoia and Shulman, 2021; Aye et al., 2022). However, millimolar dosages are consistently associated with inhibition of Complex I, which results in the activation of AMPK and its downstream pathways. Recent work examining the impact of 10 and 100  $\mu$ M metformin on primary trophoblasts demonstrates statistically significant differences in basal respiration, maximal respiration, and ATP production in primary

trophoblasts treated with vehicle or 100  $\mu$ M metformin (Tarry-Adkins et al., 2022a). While this is a different cellular model system, the absolute magnitude of respiration differences remain small and are not normalized to account for variations in cell number. In our assay, we do not detect differences in cellular respiration at the 200  $\mu$ M concentration, though profound impacts are seen at 2000  $\mu$ M concentrations. This aligns more closely with recent work demonstrating that metformin does not impact basal respiration, maximal respiration, or ATP-linked respiration at less than 1 mM in healthy syncytiotrophoblasts (Hebert and Myatt, 2023). Additionally, while we find broad changes in the relative metabolite abundance with 2000  $\mu$ M metformin treatments, we do not see similar changes between vehicle and 200  $\mu$ M metformin treatments. Overall, this suggests

that the potential benefits of metformin in pregnancy may not be attributable to large changes in trophoblast metabolism.

Prior studies have investigated metformin's impact on osteogenic, neuronal, myogenic, and adipogenic differentiation with varying results (Reviewed in (Jiang and Liu, 2020)). These reports highlight variability in metformin's impact on differentiation across multiple systems. This may be due to differences in metformin treatments or reflect inherent differences in differentiation across different cell populations. Given that GDM is associated with potential impairments in trophoblast differentiation, we examined metformin's impact on trophoblast differentiation. While supra-therapeutic levels of metformin impair trophoblast biochemical differentiation in our BeWo cell model, we do not detect impairments in differentiation at therapeutic levels of metformin in either the BeWo or trophoblast stem cell models of differentiation. This suggests that metformin may not be directly contributing to differentiation defects seen in GDM.

The mechanisms underlying 2000  $\mu$ M metformin's impact on trophoblast differentiation are not known. Prior reports have implicated AMPK activation as a regulator of trophoblast differentiation with shRNA knock-down of AMPK impairing trophoblast differentiation in the SM10 Trophoblast cell line models (Carey et al., 2014; Waker et al., 2017). It may be that higher doses of metformin modulate AMPK activity and impair differentiation in our system. Mitochondrial metabolism contributes to the epigenetic regulation of gene expression (Dai et al., 2020), and impairments in mitochondrial function at high doses of metformin may dysregulate epigenetic reprogramming during trophoblast differentiation. Human placental explants treated with 7 mM metformin demonstrated increased levels of Histone 3 Lysine 27 acetylation (Jiang et al., 2020). This highlights the potential role for supra-therapeutic concentrations of metformin to epigenetically regulate trophoblast differentiation.

For this work, we primarily relied on the BeWo model of cellular differentiation which may not fully recapitulate all aspects of trophoblast metabolism and differentiation. While this model has been extensively used to study trophoblast differentiation and exhibits many gene and hormone expression changes similar to primary trophoblasts, it may not fully represent all aspects of trophoblast differentiation (Rothbauer et al., 2017; Azar et al., 2018; Pastushek et al., 2021). For instance, BeWo cells were originally isolated from a choriocarcinoma of male lineage and are aneuploid, which may impact gene regulation and cellular metabolism (Pattillo and Gey, 1968; Weber et al., 2021). Given this limitation, we evaluated the effect of two different concentrations of metformin using a trophoblast stem cell model of differentiation derived from first trimester placenta (Okae et al., 2018). Although supra-therapeutic metformin resulted in cell death, therapeutic concentrations of metformin did not impair trophoblast differentiation, again supporting the observation that metformin is unlikely to impair trophoblast differentiation into syncytiotrophoblasts at therapeutic concentrations. Future work will assess the impact of physiologic concentrations of metformin on primary trophoblast differentiation isolated from term placenta.

Overall, this work suggests that therapeutic concentrations of metformin are not likely to strongly impact trophoblast metabolism or differentiation. Additionally, it highlights the dose-dependent impacts of metformin on cellular metabolism and differentiation

events. The potential beneficial impacts of metformin seen clinically in GDM are likely to occur independent of inhibition of complex I and trophoblast differentiation into syncytiotrophoblasts.

## Data availability statement

The raw data supporting the conclusion of this article will be made available by the authors, without undue reservation.

## Author contributions

SN and SW conceived of the study, designed and completed experiments, analyzed data, prepared figures, and wrote the manuscript. RM performed experiments, analyzed data, and prepared figures. SJ and DS performed experiments. AN, PC, and PP assisted with mass spectrometry analyses and interpretation. SJ and EA performed Seahorse experiments, analyzed, and interpreted data. MG assisted with TSC experiments and data interpretation. All authors reviewed the manuscript. All authors contributed to the article and approved the submitted version.

## Funding

SW is supported by the Reproductive Scientist Development Program (RSDP) by the Eunice Kennedy Shriver National Institute of Child Health and Human Development (K12 HD000849) and the American Board of Obstetrics and Gynecology. MG is supported by 5R21HD102770. EA is supported by R56DK131447. PC is supported by R01DK091538 and R01AG069781.

## Conflict of interest

PC has served as an external consultant for Pfizer, Inc., Abbott Laboratories, Janssen Research & Development, and Juvenesence.

The remaining authors declare that the research was conducted in the absence of any commercial or financial relationships that could be construed as a potential conflict of interest.

## Publisher's note

All claims expressed in this article are solely those of the authors and do not necessarily represent those of their affiliated organizations, or those of the publisher, the editors and the reviewers. Any product that may be evaluated in this article, or claim that may be made by its manufacturer, is not guaranteed or endorsed by the publisher.

## Supplementary material

The Supplementary Material for this article can be found online at: <https://www.frontiersin.org/articles/10.3389/fcell.2023.1167097/full#supplementary-material>

## References

- Acog Practice Bulletin No (2018). ACOG Practice Bulletin No. 190: Gestational diabetes mellitus. *Obstet. Gynecol.* 131, e49–e64. doi:10.1097/AOG.0000000000002501
- Adams, J. H., Poehlmann, J., Racine, J. L., Iruetagoiena, J. L., Eddy, A., Hoppe, K. K., et al. (2022). Weight gain in pregnancy: Can metformin steady the scales? *J. Matern. Fetal Neonatal Med.* 35, 9504–9510. doi:10.1080/14767058.2022.2044775
- Arshad, R., Kanpurwala, M. A., Karim, N., and Hassan, J. A. (2016). Effects of diet and metformin on placental morphology in gestational diabetes mellitus. *Pak J. Med. Sci.* 32, 1522–1527. doi:10.12669/pjms.326.10872
- Aye, I., Aiken, C. E., Charnock-Jones, D. S., and Smith, G. C. S. (2022). Placental energy metabolism in health and disease—significance of development and implications for preeclampsia. *Am. J. Obstet. Gynecol.* 226, S928–S944. doi:10.1016/j.ajog.2020.11.005
- Azar, C., Valentine, M., Trausch-Azar, J., Druley, T., Nelson, D. M., and Schwartz, A. L. (2018). RNA-Seq identifies genes whose proteins are transformative in the differentiation of cytotrophoblast to syncytiotrophoblast, in human primary villous and BeWo trophoblasts. *Sci. Rep.* 8, 5142. doi:10.1038/s41598-018-23379-2
- Bucher, M., Kadam, L., Ahuna, K., and Myatt, L. (2021). Differences in glycolysis and mitochondrial respiration between cytotrophoblast and syncytiotrophoblast *in vitro*: Evidence for sexual dimorphism. *Int. J. Mol. Sci.* 22, 10875. doi:10.3390/ijms221910875
- Carey, E. A., Albers, R. E., Doliboa, S. R., Hughes, M., Wyatt, C. N., Natale, D. R., et al. (2014). AMPK knockdown in placental trophoblast cells results in altered morphology and function. *Stem Cells Dev.* 23, 2921–2930. doi:10.1089/scd.2014.0092
- Chakrabarty, R. P., and Chandel, N. S. (2021). Mitochondria as signaling organelles control mammalian stem cell fate. *Cell Stem Cell* 28, 394–408. doi:10.1016/j.stem.2021.02.011
- Cheng, Y. A., Hossain, S., Trapnell, B., Kong, S., and Handwerger, S. (2004). Critical role for transcription factor AP-2alpha in human trophoblast differentiation. *Physiol. Genomics* 18, 99–107. doi:10.1152/physiolgenomics.00181.2003
- Cheung, K. S., Chan, E. W., Wong, A. Y. S., Chen, L., Seto, W. K., Wong, I. C. K., et al. (2019). Metformin use and gastric cancer risk in diabetic patients after *Helicobacter pylori* eradication. *J. Natl. Cancer Inst.* 111, 484–489. doi:10.1093/jnci/djy144
- Costa, M. A. (2016). Scrutinising the regulators of syncytialization and their expression in pregnancy-related conditions. *Mol. Cell Endocrinol.* 420, 180–193. doi:10.1016/j.mce.2015.11.010
- D'ambrosio, V., Brunelli, R., Vena, F., Di Mascio, D., Marchetti, C., Boccherini, C., et al. (2019). Metformin reduces maternal weight gain in obese pregnant women: A systematic review and meta-analysis of two randomized controlled trials. *Diabetes Metab. Res. Rev.* 35, e3164. doi:10.1002/dmrr.3164
- Dadwal, P., Mahmud, N., Sinai, L., Azimi, A., Fatt, M., Wondisford, F. E., et al. (2015). Activating endogenous neural precursor cells using metformin leads to neural repair and functional recovery in a model of childhood brain injury. *Stem Cell Rep.* 5, 166–173. doi:10.1016/j.stemcr.2015.06.011
- Dai, Z., Ramesh, V., and Locasale, J. W. (2020). The evolving metabolic landscape of chromatin biology and epigenetics. *Nat. Rev. Genet.* 21, 737–753. doi:10.1038/s41576-020-0270-8
- Elsayed, N. A., Aleppo, G., Aroda, V. R., Bannuru, R. R., Brown, F. M., Bruemmer, D., et al. (2023). 9. Pharmacologic approaches to glycemic treatment: Standards of care in diabetes-2023. *Diabetes Care* 46, S140–S157. doi:10.2337/dc23-S009
- Folmes, C. D., and Terzic, A. (2016). Energy metabolism in the acquisition and maintenance of stemness. *Semin. Cell Dev. Biol.* 52, 68–75. doi:10.1016/j.semcdb.2016.02.010
- Fournier, T., Guibourdenche, J., and Evain-Brion, D. (2015). Review: hCGs: Different sources of production, different glycoforms and functions. *Placenta* 36 (1), S60–S65. doi:10.1016/j.placenta.2015.02.002
- Hebert, J. F., and Myatt, L. (2023). Metformin impacts human syncytiotrophoblast mitochondrial function from pregnancies complicated by obesity and gestational diabetes mellitus in a sexually dimorphic manner. *Antioxidants (Basel)* 12.
- Higgins, L., Greenwood, S. L., Wareing, M., Sibley, C. P., and Mills, T. A. (2011). Obesity and the placenta: A consideration of nutrient exchange mechanisms in relation to aberrant fetal growth. *Placenta* 32, 1–7. doi:10.1016/j.placenta.2010.09.019
- Huynh, J., Yamada, J., Beauharnais, C., Wenger, J. B., Thadhani, R. I., Wexler, D., et al. (2015). Type 1, type 2 and gestational diabetes mellitus differentially impact placental pathologic characteristics of uteroplacental malperfusion. *Placenta* 36, 1161–1166. doi:10.1016/j.placenta.2015.08.004
- Ivanisevic, J., Zhu, Z. J., Plate, L., Tautenhahn, R., Chen, S., O'Brien, P. J., et al. (2013). Toward 'omic scale metabolite profiling: A dual separation-mass spectrometry approach for coverage of lipid and central carbon metabolism. *Anal. Chem.* 85, 6876–6884. doi:10.1021/ac401140h
- Jaiman, S., Romero, R., Pacora, P., Jung, E., Bhatti, G., Yeo, L., et al. (2020). Disorders of placental villous maturation in fetal death. *J. Perinat. Med.* 1. doi:10.1515/jpm-2020-0030
- Jiang, L. L., and Liu, L. (2020). Effect of metformin on stem cells: Molecular mechanism and clinical prospect. *World J. Stem Cells* 12, 1455–1473. doi:10.4252/wjsc.v12.i12.1455
- Jiang, S., Teague, A. M., Tryggestad, J. B., Jensen, M. E., and Chernausk, S. D. (2020). Role of metformin in epigenetic regulation of placental mitochondrial biogenesis in maternal diabetes. *Sci. Rep.* 10, 8314. doi:10.1038/s41598-020-65415-0
- Karahoda, R., Zaugg, J., Fuenzalida, B., Kallol, S., Moser-Haessig, R., Staud, F., et al. (2022). Trophoblast differentiation affects crucial nutritive functions of placental membrane transporters. *Front. Cell Dev. Biol.* 10, 820286. doi:10.3389/fcell.2022.820286
- Khong, T. Y., Mooney, E. E., Ariel, I., Balmus, N. C., Boyd, T. K., Brundler, M. A., et al. (2016). Sampling and definitions of placental lesions: Amsterdam placental workshop group consensus statement. *Arch. Pathol. Lab. Med.* 140, 698–713. doi:10.5858/arpa.2015-0225-CC
- Kolahi, K. S., Valent, A. M., and Thornburg, K. L. (2017). Cytotrophoblast, not syncytiotrophoblast, dominates glycolysis and oxidative phosphorylation in human term placenta. *Sci. Rep.* 7, 42941. doi:10.1038/srep42941
- Lager, S., and Powell, T. L. (2012). Regulation of nutrient transport across the placenta. *J. Pregnancy* 2012, 179827. doi:10.1155/2012/179827
- Lamoia, T. E., and Shulman, G. I. (2021). Cellular and molecular mechanisms of metformin action. *Endocr. Rev.* 42, 77–96. doi:10.1210/edrv/bnaa023
- Leduc, K., Bourassa, V., Asselin, E., Leclerc, P., Lafond, J., and Reyes-Moreno, C. (2012). Leukemia inhibitory factor regulates differentiation of trophoblastlike BeWo cells through the activation of JAK/STAT and MAPK3/1 MAP kinase-signaling pathways. *Biol. Reprod.* 86, 54. doi:10.1095/biolreprod.111.094334
- Liang, H. L., Ma, S. J., Xiao, Y. N., and Tan, H. Z. (2017). Comparative efficacy and safety of oral antidiabetic drugs and insulin in treating gestational diabetes mellitus: An updated PRISMA-compliant network meta-analysis. *Med. Baltim.* 96, e7939. doi:10.1097/MD.00000000000007939
- Lisowski, P., Kannan, P., Mlody, B., and Prigione, A. (2018). Mitochondria and the dynamic control of stem cell homeostasis. *EMBO Rep.* 19, e45432. doi:10.15252/embr.201745432
- Løvvik, T. S., Carlsen, S. M., Salvesen, Ø., Steffensen, B., Bixo, M., Gómez-Real, F., et al. (2019). Use of metformin to treat pregnant women with polycystic ovary syndrome (PregMet2): A randomised, double-blind, placebo-controlled trial. *Lancet Diabetes Endocrinol.* 7, 256–266. doi:10.1016/S2213-8587(19)30002-6
- Maruthur, N. M., Tseng, E., Hutflless, S., Wilson, L. M., Suarez-Cuervo, C., Berger, Z., et al. (2016). Diabetes medications as monotherapy or metformin-based combination therapy for type 2 diabetes: A systematic review and meta-analysis. *Ann. Intern. Med.* 164, 740–751. doi:10.7326/M15-2650
- Musi, N., and Goodyear, L. J. (2002). Targeting the AMP-activated protein kinase for the treatment of type 2 diabetes. *Curr. Drug Targets Immune Endocr. Metabol. Disord.* 2, 119–127. doi:10.2174/1568005310202020119
- Okae, H., Toh, H., Sato, T., Hiura, H., Takahashi, S., Shirane, K., et al. (2018). Derivation of human trophoblast stem cells. *Cell Stem Cell* 22, 50–63. doi:10.1016/j.stem.2017.11.004
- Omata, W., Ackerman, W. E. T., Vandre, D. D., and Robinson, J. M. (2013). Trophoblast cell fusion and differentiation are mediated by both the protein kinase C and a pathways. *PLoS One* 8, e81003. doi:10.1371/journal.pone.0081003
- Orendi, K., Gauster, M., Moser, G., Meiri, H., and Huppertz, B. (2010). The choriocarcinoma cell line BeWo: Syncytial fusion and expression of syncytium-specific proteins. *Reproduction* 140, 759–766. doi:10.1530/REP-10-0221
- Orendi, K., Kivity, V., Sammar, M., Grimpel, Y., Gonen, R., Meiri, H., et al. (2011). Placental and trophoblastic *in vitro* models to study preventive and therapeutic agents for preeclampsia. *Placenta* 32, S49–S54. doi:10.1016/j.placenta.2010.11.023
- Pastuschek, J., Nonn, O., Gutierrez-Samudio, R. N., Murrieta-Coxca, J. M., Muller, J., Sanft, J., et al. (2021). Molecular characteristics of established trophoblast-derived cell lines. *Placenta* 108, 122–133. doi:10.1016/j.placenta.2021.02.022
- Pattillo, R. A., and Gey, G. O. (1968). The establishment of a cell line of human hormone-synthesizing trophoblastic cells *in vitro*. *Cancer Res.* 28, 1231–1236.
- Puchalska, P., Huang, X., Martin, S. E., Han, X., Patti, G. J., and Crawford, P. A. (2018). Isotope tracing untargeted metabolomics reveals macrophage polarization-state-specific metabolic coordination across intracellular compartments. *iScience* 9, 298–313. doi:10.1016/j.isci.2018.10.029
- Puchalska, P., Martin, S. E., Huang, X., Lengfeld, J. E., Daniel, B., Graham, M. J., et al. (2019). Hepatocyte-macrophage acetoacetate shuttle protects against tissue fibrosis. *Cell Metab.* 29, 383–398. doi:10.1016/j.cmet.2018.10.015
- Rena, G., Hardie, D. G., and Pearson, E. R. (2017). The mechanisms of action of metformin. *Diabetologia* 60, 1577–1585. doi:10.1007/s00125-017-4342-z
- Renaud, S. J., and Jeyarajah, M. J. (2022). How trophoblasts fuse: An in-depth look into placental syncytiotrophoblast formation. *Cell Mol. Life Sci.* 79, 433. doi:10.1007/s00018-022-04475-z

- Rothbauer, M., Patel, N., Gondola, H., Siwetz, M., Huppertz, B., and Ertl, P. (2017). A comparative study of five physiological key parameters between four different human trophoblast-derived cell lines. *Sci. Rep.* 7, 5892. doi:10.1038/s41598-017-06364-z
- Senesi, P., Montesano, A., Luzi, L., Codella, R., Benedini, S., and Terruzzi, I. (2016). Metformin treatment prevents sedentariness related damages in mice. *J. Diabetes Res.* 2016, 8274689. doi:10.1155/2016/8274689
- Syngelaki, A., Nicolaidis, K. H., Balani, J., Hyer, S., Akolekar, R., Kotecha, R., et al. (2016). Metformin versus placebo in obese pregnant women without diabetes mellitus. *N. Engl. J. Med.* 374, 434–443. doi:10.1056/NEJMoa1509819
- Tan, W., Tang, H., Jiang, X., Ye, F., Huang, L., Shi, D., et al. (2019). Metformin mediates induction of miR-708 to inhibit self-renewal and chemoresistance of breast cancer stem cells through targeting CD47. *J. Cell Mol. Med.* 23, 5994–6004. doi:10.1111/jcmm.14462
- Tarry-Adkins, J. L., Aiken, C. E., and Ozanne, S. E. (2019). Neonatal, infant, and childhood growth following metformin versus insulin treatment for gestational diabetes: A systematic review and meta-analysis. *PLoS Med.* 16, e1002848. doi:10.1371/journal.pmed.1002848
- Tarry-Adkins, J. L., Robinson, I. G., Reynolds, R. M., Aye, I., Charnock-Jones, D. S., Jenkins, B., et al. (2022a). Impact of metformin treatment on human placental energy production and oxidative stress. *Front. Cell Dev. Biol.* 10, 935403. doi:10.3389/fcell.2022.935403
- Tracy, A., Higgins, M., Kearney, J. M., Mcauliffe, F., and Mooney, E. E. (2013). Delayed villous maturation of the placenta: Quantitative assessment in different cohorts. *Pediatr. Dev. Pathol.* 16, 63–66. doi:10.2350/12-06-1218-OA.1
- Turco, M. Y., and Moffett, A. (2019). Development of the human placenta. *Development* 146. doi:10.1242/dev.163428
- Waker, C. A., Albers, R. E., Pye, R. L., Doliboa, S. R., Wyatt, C. N., Brown, T. L., et al. (2017). AMPK knockdown in placental labyrinthine progenitor cells results in restriction of critical energy resources and terminal differentiation failure. *Stem Cells Dev.* 26, 808–817. doi:10.1089/scd.2016.0252
- Wang, J., Gallagher, D., Devito, L. M., Cancino, G. I., Tsui, D., He, L., et al. (2012). Metformin activates an atypical PKC-CBP pathway to promote neurogenesis and enhance spatial memory formation. *Cell Stem Cell* 11, 23–35. doi:10.1016/j.stem.2012.03.016
- Weber, M., Weise, A., Vashghani, F., Gohner, C., Fitzgerald, J. S., Liehr, T., et al. (2021). Cytogenomics of six human trophoblastic cell lines. *Placenta* 103, 72–75. doi:10.1016/j.placenta.2020.10.011
- Zhao, B., Luo, J., Wang, Y., Zhou, L., Che, J., Wang, F., et al. (2019). Metformin suppresses self-renewal ability and tumorigenicity of osteosarcoma stem cells via reactive oxygen species-mediated apoptosis and autophagy. *Oxid. Med. Cell Longev.* 2019, 9290728. doi:10.1155/2019/9290728